# Control of cytoskeletal dynamics during cellular responses to pore forming toxins

Francisco Sarmento Mesquita [1,2,*], Cláudia Brito [1,2,3], Didier Cabanes [1,2], Sandra Sousa [1,2,*]

[1]i3S-Instituto de Investigação e Inovação em Saúde, Universidade do Porto, Rua Alfredo Allen 208, 4200-135 Porto, Portugal

[2]Group of Molecular Microbiology, IBMC, Universidade do Porto, Rua Alfredo Allen 208, 4200-135 Porto, Portugal

[3]Instituto de Ciências Biomédicas Abel Salazar (ICBAS), Universidade do Porto, Rua Jorge de Viterbo Ferreira 228, 4050-343 Porto, Portugal

[*]corresponding author: Francisco Sarmento Mesquita (francisco.mesquita@ibmc.up.pt) and Sandra Sousa (srsousa@ibmc.up.pt)

**Abstract**

Following damage by pore forming toxins (PFTs) host cells engage repair processes and display profound cytoskeletal remodeling and concomitant plasma membrane (PM) blebbing. We have recently demonstrated that host cells utilise similar mechanisms to control cytoskeletal dynamics in response to PFTs and during cell migration. This involves assembly of cortical actomyosin bundles, reorganisation of the endoplasmic reticulum (ER) network, and the interaction between the ER chaperone Gp96 and the molecular motor Non-muscle Myosin Heavy Chain IIA (NMHCIIA). Consequently, Gp96 regulates actomyosin activity, PM blebbing and cell migration, and protects PM integrity against PFTs. In addition, we observed that PFTs increase association of Gp96 and ER vacuoles with the cell surface or within PM blebs loosely attached to the cell body. Similarly, gut epithelial cells damaged by PFTs *in vivo* were shown to release microvilli structures or directly purge cytoplasmic content. Cytoplasmic purging involves profound cytoskeletal remodeling and ER vacuolation, suggesting that our observations recapitulate recovery processes *in vivo*. Here, we discuss our findings in light of the current understanding of PM repair mechanisms and *in vivo* recovery responses to PFTs.

**Keywords**

plasma membrane repair; actomyosin; endoplasmic reticulum chaperone; blebbing; pore-forming toxin; listeriolysin O

**Original article:**

Mesquita FS, Brito C, Mazon Moya MJ, Pinheiro JC, Mostowy S, Cabanes D, Sousa S (2017) Endoplasmic reticulum chaperone Gp96 controls actomyosin dynamics and protects against pore-forming toxins. *EMBO Rep* **18:** 303-318

## Introduction

Evolutionary conserved mechanisms allow eukaryotic cells to sustain mechanical and chemical stress that injure the PM[1-3]. The changes in the intracellular concentration of calcium and potassium caused by PM rupture initiate recovery processes which depend on the size of the damage, the cell types involved and the nature of the inflicted stress (e.g. mechanical injuries or insertion of stable protein pores such as those created by bacterial PFTs)[1-3]. In general, cells engage PM repair pathways, rearrange the cytoskeleton, control their metabolic state and activate stress-associated signalling[2, 3].

PM damage promotes calcium influx, which enhances exocytosis, predominantly of lysosomes. These vesicles patch large mechanical wounds (>100 nm)[4], and promote acid-sphingomyelinase (ASM) release, which generates PM-ceramide domains that engulf PM damage in caveolae-derived endosomes[2, 5]. Stable protein pores cannot be patched and are removed by endocytosis or shedding within small PM vesicles (nm size)[6]. PM shedding may actually constitute an intrinsic repair mechanism that senses PFT oligomerisation and is potentiated upon damage and calcium influx[7]. Shedding depends on endosomal sorting complexes required for transport (ESCRT) and is similar to the budding of viral particles[6-8]. *In vivo*, recovery from PFT-mediated damage appears to involve the cooperation between different mechanisms. Host survival requires regulators of both endocytic and exocytic trafficking and epithelial cells display increased rates of endocytosis, shedding of PM material[9] and/or direct purging of cytoplasmic content[10]. In addition, epithelia compact its cytoskeletal network and display alterations of cellular organelles while preserving coherence and functionality[10]. The fine control of the cytoskeletal dynamics is therefore necessary to promote PM recovery[11]. Indeed, following mechanically-induced PM damage, microtubules allow recruitment of distal vesicles while local actin rearrangements and myosin activity relief tension facilitate vesicle delivery and provide force to re-establish PM integrity[12-16]. The importance of cytoskeletal dynamics in cells targeted by PFTs remains poorly defined.

## Novel regulators of cytoskeletal dynamics protect against PFTs

We recently identified the ER chaperone Gp96 and NMHCIIA as regulators of cytoskeletal dynamics following PFT-mediated PM damage[17]. Gp96 and NMHCIIA interact upon PFT intoxication and accumulate into distinct bundles at sites of PM blebbing (Figure 1 and Supp Mov 1)[17]. These processes require calcium influx generated by PM damage and occur during *Listeria monocytogenes* (*Lm*) infection, which depends on the PFT listeriolysin O (LLO). The reorganisation of the actomyosin network is mediated by Gp96, which modulates myosin II activity and coordinates PM blebbing during PFT intoxication. Both Gp96 and NMHCIIA promote cell survival upon LLO intoxication[17].

We characterised further the formation of NMHCIIA bundles during PFT intoxication and found that host cells utilise similar mechanisms to regulate cytoskeletal dynamics during recovery of PM integrity and cell migration[17]. (i) PFT-induced actomyosin bundles accumulate proteins found at the trailing edge

of migrating cells[18, 19]; (ii) upon PFT intoxication, Gp96 interacts with Filamin-A, an actin cross-linker that regulates cell migration[20]; and (iii) stimulation of cell migration with Wnt5a, which promotes assembly of rear-end ER-actomyosin structures, also enhances NMHCIIA-Gp96 interaction. In line with these observations, we showed that Gp96 regulates general cytoskeletal organisation and therefore modulates cell shape and cell motility[17].

Recent independent studies have also proposed a role for Gp96 in cytoskeletal organisation, cell polarity and cell migration. This may occur through the control of vesicular trafficking and/or interaction with different cytoskeletal proteins such as F-actin-capping protein 1, Actin, Radixin and ROCK2[21, 22]. Of note, Gp96 is predominantly expressed at early stages of development and contributes to the establishment of epithelial gut morphology and apical specification[23]. Polarised lysosome secretion and establishment of cell polarity are regulated by NMHCIIA[14, 24]. Therefore, it is possible that Gp96 and NMHCIIA interact to coordinate vesicular trafficking and cytoskeletal dynamics necessary for the definition of cell polarity and for efficient PM repair. Whether NMHCIIA and Gp96 directly interact remains unknown. Yet, Gp96 is the ER paralogue of the cytosolic chaperone HSP90, which binds myosin head domains and is necessary to coordinate assembly and folding of myosin thick filaments[25].

Few additional molecules were associated with the cytoskeletal reorganisation following PFT-mediated PM damage. RhoA and Rac1 GTPases promote actin remodelling[26] and Src-family kinases mediate microtubule bundling and stabilisation[27]. The importance of such processes for cell recovery from PFT-mediated wounding is uncertain. Nevertheless, GTPases (RhoA, Rac and Cdc42) coordinate the assembly and dynamics of actomyosin rings, which promote closure of laser-induced wounds in *Xenopus* oocytes[28], and Src, together with myosin light chain kinase (MLCK), regulate PM expansion during osmotic stress[29].

Besides actomyosin reorganisation and simultaneous PM blebbing, cells modify the entire ER network following PFT intoxication[17], as depicted by the alteration of the characteristic ER reticular pattern and formation of vacuoles containing mCherry-Sec61β (a subunit of the ER membrane translocon complex Sec61) (Figure 1 and Supp Mov 1). Vacuolation of the ER and other cellular organelles has been reported in response to different PFTs in various cell types and *in vivo*[1, 10]. The relevance of such morphological alteration is not understood and has been mainly associated with organelle damage and cell death[1]. However, following toxin wash-out, cells recover normal actomyosin and ER distribution with equivalent kinetics[17].

Lysosomes and the ER are major intracellular calcium stores and their dynamics are crucial for functioning. In particular, the transient distribution of ER and lysosomes to the trailing edge of migrating cells directs calcium signalling and assembly of cytoskeletal complexes that mediate tail retraction[18]. Of note, stimulation of such process enhances Gp96-NMHCIIA interaction[17]. However, the role of the ER during recovery from PFT-induced PM damage remains unclear. ER proteins have been detected at PM wounds of mechanically injured cells[30] and inhibition of ER stress pathways or calcium sequestration

compromises survival after PFT intoxication[31, 32]. Whether lysosomes or the ER control calcium signalling and actomyosin dynamics during PM repair is still speculation[30]. Nevertheless, Gp96 regulates calcium homeostasis at the ER[33].

We observed that certain LLO-intoxicated cells appear to expose ER compartments containing ER-retention sequence KDEL, Gp96 and Sec61α at the cell surface or within large PM blebs loosely attached to the cell body (Figure 2A-C)[17]. Transmission electron microscopy (TEM) of intoxicated HeLa cells confirmed that such vacuoles are detected within large bleb-like structures at the proximity of the PM and apparently detached from the cell body (Figure 2D). Thus, upon damage, cells can release ER-derived compartments to the extracellular environment. Whether the release of ER vacuoles only occurs in dying cells or upon organelle damage is still unclear. Yet these processes may constitute a common feature of cellular responses to PFTs, since targeting of gut epithelial cells by PFTs *in vivo* induces release of microvilli structures, cytosolic purging, ER vacuolation and rearrangement of the cellular cytoskeleton[9, 10].

PFT-induced PM blebbing was considered to be protective and distinct from PM shedding of PFT pores within small vesicles (nm size). Large transient blebs (µm size) presumably promote PM repair by buffering injured sites, preventing excess calcium influx and loss of cytosolic content[2, 3, 6, 34]. Blebs can be shed and, during apoptosis, permeabilisation of PM blebs enables the release of cytosolic content [35, 36]. Thus, it is possible that cytosolic purging and PM blebbing are complementary processes. Finally, increasing evidence supports a role for extruded vesicles during bacterial infections. While some studies have suggested that microvesicle release or cytosolic purging may favour elimination of intracellular bacteria[10, 37, 38], certain bacteria, such as *Lm,* where propose to disseminate within large bleb-like structures[39, 40].

**Conclusion and future perspectives**

We have highlighted the importance of NMHCIIA and uncovered an unexpected role for the ER chaperone Gp96 in host cell recovery against PFTs. Future studies are now necessary to understand how cytoskeletal dynamics interfere with polarised secretion and shedding of cellular material, which protect host tissues from PFT attack. Moreover, it will be important to further analyse the physiological relevance of recovery mechanisms in the context of bacterial infections: What are the consequences of PM blebbing and cytosolic purging in the context of different infections? Are these processes related to the shedding of apoptotic bodies and damaged cells from infected epithelia?

As PM recovery processes display important evolutionary conserved features[2, 3, 11], the ground-breaking use of amenable models such as zebrafish (*Danio rerio*) and drosophila (*Drosophila melanogaster*) to the direct visualization of infectious processes *in vivo* will continue to be of critical importance[10, 17].

**Acknowledgements**

This work was supported by national funds through FCT - Fundação para a Ciência e a Tecnologia / MEC - Ministério da Educação e Ciência and co-funded by FEDER-COMPETE 2020 and NORTE 2020 within projects POCI-01-0145-FEDER-007274, NORTE-01-0145-FEDER-000012 and Infect ERA/0001/2013 PROANTILIS. F.S.M. and C.B. were supported by FCT fellowships (SFRH/BPD/94458/2013, SFRH/BD/112217/2015). SS received supported from FCT Investigator program (COMPETE, POPH, and FCT).

**References**


1. Bischofberger, M., Iacovache, I. & van der Goot, F.G. Pathogenic pore-forming proteins: function and host response. *Cell Host Microbe* **12**, 266-275 (2012).
2. Andrews, N.W., Almeida, P.E. & Corrotte, M. Damage control: cellular mechanisms of plasma membrane repair. *Trends Cell Biol* **24**, 734-742 (2014).
3. Cooper, S.T. & McNeil, P.L. Membrane Repair: Mechanisms and Pathophysiology. *Physiol Rev* **95**, 1205-1240 (2015).
4. McNeil, P.L., Vogel, S.S., Miyake, K. & Terasaki, M. Patching plasma membrane disruptions with cytoplasmic membrane. *J Cell Sci* **113 ( Pt 11)**, 1891-1902 (2000).
5. Tam, C. *et al.* Exocytosis of acid sphingomyelinase by wounded cells promotes endocytosis and plasma membrane repair. *J Cell Biol* **189**, 1027-1038 (2010).
6. Jimenez, A.J. *et al.* ESCRT machinery is required for plasma membrane repair. *Science* **343**, 1247136 (2014).
7. Romero, M. *et al.* Intrinsic repair protects cells from pore-forming toxins by microvesicle shedding. *Cell Death Differ* (2017).
8. Keyel, P.A. *et al.* Streptolysin O clearance through sequestration into blebs that bud passively from the plasma membrane. *J Cell Sci* **124**, 2414-2423 (2011).
9. Los, F.C. *et al.* RAB-5- and RAB-11-dependent vesicle-trafficking pathways are required for plasma membrane repair after attack by bacterial pore-forming toxin. *Cell Host Microbe* **9**, 147-157 (2011).
10. Lee, K.-Z. *et al.* Enterocyte Purge and Rapid Recovery Is a Resilience Reaction of the Gut Epithelium to Pore-Forming Toxin Attack. *Cell Host Microbe* **20**, 716-730 (2016).
11. Boucher, E. & Mandato, C.A. Plasma membrane and cytoskeleton dynamics during single-cell wound healing. *Biochim Biophys Acta* **1853**, 2649-2661 (2015).
12. Miyake, K., McNeil, P.L., Suzuki, K., Tsunoda, R. & Sugai, N. An actin barrier to resealing. *J Cell Sci* **114**, 3487-3494 (2001).
13. Togo, T. & Steinhardt, R.A. Nonmuscle myosin IIA and IIB have distinct functions in the exocytosis-dependent process of cell membrane repair. *Mol Biol Cell* **15**, 688-695 (2004).
14. Encarnacao, M. *et al.* A Rab3a-dependent complex essential for lysosome positioning and plasma membrane repair. *J Cell Biol* **213**, 631-640 (2016).
15. Mandato, C.A. & Bement, W.M. Actomyosin transports microtubules and microtubules control actomyosin recruitment during Xenopus oocyte wound healing. *Curr Biol* **13**, 1096-1105 (2003).
16. Togo, T. Disruption of the plasma membrane stimulates rearrangement of microtubules and lipid traffic toward the wound site. *J Cell Sci* **119**, 2780-2786 (2006).
17. Mesquita, F.S. *et al.* Endoplasmic reticulum chaperone Gp96 controls actomyosin dynamics and protects against pore-forming toxins. *EMBO Rep* **18**, 303-318 (2017).
18. Witze, E.S. *et al.* Wnt5a directs polarized calcium gradients by recruiting cortical endoplasmic reticulum to the cell trailing edge. *Dev Cell* **26**, 645-657 (2013).
19. Sanchez-Madrid, F. & Serrador, J.M. Bringing up the rear: defining the roles of the uropod. *Nat Rev Mol Cell Biol* **10**, 353-359 (2009).
20. Razinia, Z., Makela, T., Ylanne, J. & Calderwood, D.A. Filamins in mechanosensing and signaling. *Annu Rev Biophys* **41**, 227-246 (2012).
21. Hong, F. *et al.* Mapping the Interactome of a Major Mammalian Endoplasmic Reticulum Heat Shock Protein 90. *PLoS One* **12**, e0169260 (2017).
22. Ghosh, S., Shinogle, H.E., Galeva, N.A., Dobrowsky, R.T. & Blagg, B.S.J. Endoplasmic Reticulum-resident Heat Shock Protein 90 (HSP90) Isoform Glucose-regulated Protein 94 (GRP94) Regulates Cell Polarity and Cancer Cell Migration by Affecting Intracellular Transport. *J Biol Chem* **291**, 8309-8323 (2016).
23. Maynard, J.C. *et al.* Gp93, the Drosophila GRP94 ortholog, is required for gut epithelial homeostasis and nutrient assimilation-coupled growth control. *Dev Biol* **339**, 295-306 (2010).
24. Vicente-Manzanares, M., Ma, X., Adelstein, R.S. & Horwitz, A.R. Non-muscle myosin II takes centre stage in cell adhesion and migration. *Nat Rev Mol Cell Biol* **10**, 778-790 (2009).
25. Hellerschmied, D. & Clausen, T. Myosin chaperones. *Curr Opin Struct Biol* **25**, 9-15 (2014).

26. Iliev, A.I., Djannatian, J.R., Nau, R., Mitchell, T.J. & Wouters, F.S. Cholesterol-dependent actin remodeling via RhoA and Rac1 activation by the Streptococcus pneumoniae toxin pneumolysin. *Proc Natl Acad Sci U S A* **104**, 2897-2902 (2007).
27. Iliev, A.I. *et al.* Rapid microtubule bundling and stabilization by the Streptococcus pneumoniae neurotoxin pneumolysin in a cholesterol-dependent, non-lytic and Src-kinase dependent manner inhibits intracellular trafficking. *Mol Microbiol* **71**, 461-477 (2009).
28. Abreu-Blanco, M.T., Verboon, J.M. & Parkhurst, S.M. Coordination of Rho family GTPase activities to orchestrate cytoskeleton responses during cell wound repair. *Curr Biol* **24**, 144-155 (2014).
29. Barfod, E.T., Moore, A.L., Van de Graaf, B.G. & Lidofsky, S.D. Myosin light chain kinase and Src control membrane dynamics in volume recovery from cell swelling. *Mol Biol Cell* **22**, 634-650 (2011).
30. Mellgren, R.L. A plasma membrane wound proteome: reversible externalization of intracellular proteins following reparable mechanical damage. *J Biol Chem* **285**, 36597-36607 (2010).
31. Wolfmeier, H. *et al.* $Ca^{+}$-dependent repair of pneumolysin pores: A new paradigm for host cellular defense against bacterial pore-forming toxins. *Biochim Biophys Acta* **1853**, 2045-2054 (2015).
32. Bischof, L.J. *et al.* Activation of the unfolded protein response is required for defenses against bacterial pore-forming toxin in vivo. *PLoS Pathog* **4**, e1000176 (2008).
33. Ansa-Addo, E.A. *et al.* Clients and Oncogenic Roles of Molecular Chaperone gp96/grp94. *Curr Top Med Chem* **16**, 2765-2778 (2016).
34. Babiychuk, E.B., Monastyrskaya, K., Potez, S. & Draeger, A. Blebbing confers resistance against cell lysis. *Cell Death Differ* **18**, 80-89 (2011).
35. Atanassoff, A.P. *et al.* Microvesicle shedding and lysosomal repair fulfill divergent cellular needs during the repair of streptolysin O-induced plasmalemmal damage. *PLoS One* **9**, e89743 (2014).
36. Wickman, G.R. *et al.* Blebs produced by actin-myosin contraction during apoptosis release damage-associated molecular pattern proteins before secondary necrosis occurs. *Cell Death Differ* **20**, 1293-1305 (2013).
37. Miao, Y., Li, G., Zhang, X., Xu, H. & Abraham, S.N. A TRP Channel Senses Lysosome Neutralization by Pathogens to Trigger Their Expulsion. *Cell* **161**, 1306-1319 (2015).
38. Capasso, D. *et al.* Elimination of Pseudomonas aeruginosa through Efferocytosis upon Binding to Apoptotic Cells. *PLoS Pathog* **12**, e1006068 (2016).
39. Czuczman, M.A. *et al.* Listeria monocytogenes exploits efferocytosis to promote cell-to-cell spread. *Nature* **509**, 230-234 (2014).
40. Zuck, M., Ellis, T., Venida, A. & Hybiske, K. Extrusions are phagocytosed and promote Chlamydia survival within macrophages. *Cell Microbiol* **19** (2017).

## Materials and Methods

### Plasmids and antibodies

Plasmid GFPNMHCIIA (#11347) was obtained from Addgene and mCherry-Sec61-N-18 was a gift from M. Davidson through Addgene (# 55130). Rabbit anti-NMHCIIA (Sigma); mouse anti-NMHCIIA (Abcam); rat anti-Gp96 (Enzo); mouse anti-Sec61α G-2 (Santa Cruz) were used at 1/200 for immunofluorescence microscopy (IF). PM was labelled with FITC-conjugated WGA (Sigma) DNA with 4',6-Diamidino-2-phenylindole dihydrochloride, DAPI (Sigma) and IF fluorescently-conjugated secondary antibodies (Invitrogen) were used at 1/500.

### Cell Lines and Toxin

HeLa (ATCC CCL-2) cells were cultivated in DMEM with glucose and L-glutamine, supplemented with 10% FBS. Cells were maintained at 37 °C in a 5% $CO_2$ atmosphere. Cell culture media and supplements were from Lonza. LLO was purified as previously [17] and treatments and washes were carried in Hank's Balanced Salt Solution (HBSS) as indicated.

### Immunofluorescence Microscopy

Cells were fixed in 3% paraformaldehyde (15 min), quenched with 20 mM $NH_4Cl$ (1 h), permeabilized with 0.1% Triton X-100 (5 min), and blocked with 10% BSA in PBS (30 min). Antibodies were diluted in PBS containing 1% BSA. Coverslips were incubated for 1 h with primary antibodies, washed three times in PBS and incubated 45 min with secondary antibodies. DNA was counterstained with DAPI (Sigma). Coverslips were mounted onto microscope slides with Aqua-Poly/Mount (Polysciences). Images were collected with a confocal laser-scanning microscope (Leica SP5II) and processed using ImageJ64 or Adobe Photoshop software.

### Live imaging and quantification of PM blebbing of LLO-treated cells

Cells seeded into Ibitreat µ-dishes (Ibidi), simultaneously transfected with GFPNMHCIIA and mcherrySEC61, maintained in HBSS at 37°C with 5% $CO_2$ were imaged using an Andor Revolution XD Spinning-disk confocal system with an EMCCD iXonEM+ camera, 488 nm lase lines, and a Yokogawa CSU-22 unit on an inverted microscope (IX81; Olympus), driven by Andor IQ live-cell imaging software. LLO (0.5 nM) was added 10 min after initial image acquisition. Differential interference contrast (DIC) images and GFP fluorescent datasets with 0.5 µm Z-steps were acquired using a UPLSAPO 100x/1.40 objective lens every 15 sec. ImajeJ64 was used for image sequence analysis and video assembly.

**Figure Legends**

**Figure 1 – Redistribution of NMHCIIA and ER network upon LLO treatment**

Sequential frames of time-lapse confocal microscopy sequence of LLO-treated HeLa cells expressing simultaneously GFPNMHCIIA and mCherrySec61. LLO was added to culture medium 10 seconds before t0. DIC – differential interference contrast. Highlighted inset depicts ER structures within NMHCIIA bundles and PM blebs.

**Figure 2 – Exposure of ER and Gp96 at blebs from LLO treated cells**

(**A**) Confocal microscopy Z-stack projections of HeLa cells treated with LLO (0.5 nM, 15 min) and immunolabelled for the C-terminal sequence present in ER resident proteins, ER-KDEL (red), NMHCIIA (green) and stained with DAPI (blue). Orthogonal views and 3D projections illustrate exposure of ER vacuoles at the cell surface (arrow). (**B-C**) Confocal microscopy images of HeLa cells left untreated or treated with LLO and immunolabelled for **(B)** ER-Gp96 (blue), NMHCIIA (green) and stained with FITCWGA (Plasma membrane, PM-red) and DAPI (white), or **(C)** Sec61 (red), NMHCIIA (blue) and stained with FITCWGA (green) and DAPI (white). Insets and arrows indicate NMHCIIA-positive PM blebs containing Gp96 or Sec61, loosely attached to the cell body. Arrow-heads show cortical NMHCIIA-Sec61 within the cell body. All scale bars are 10 μm. **(D)** Longitudinal TEM images of HeLa cells left untreated or treated with 0.5 nM LLO for 15 min. ER - ER cisternae in untreated cells and ER vacuoles in LLO-treated cells; N - nucleus. Arrows show vesicles and bleb-like structures at the proximity of the PM containing ER vacuoles and apparently detached from the cell body.

**Supplementary Movie 1 - NMHCIIA and ER rearrangements during PFT-induced PM blebbing**

Time-lapse confocal microscopy analysis of LLO-treated HeLa cells expressing simultaneously GFPNMHCIIA and mCherrySec61 used in Figure 1. Sequential frames were acquired every 15 seconds (10 frames per second display rate). LLO was added to culture medium 10 seconds before t0. Scale bar - 10 μm. DIC – differential interference contrast. GFPNMHIIA fluorescence image corresponds to a z-stack projection. Inset highlight depict sites where NMHCIIA bundles occur where it is possible to observe association between ER structures and NMHCIIA bundles.

Figure 2 – Exposure of ER within blebs from LLO intoxicated cells

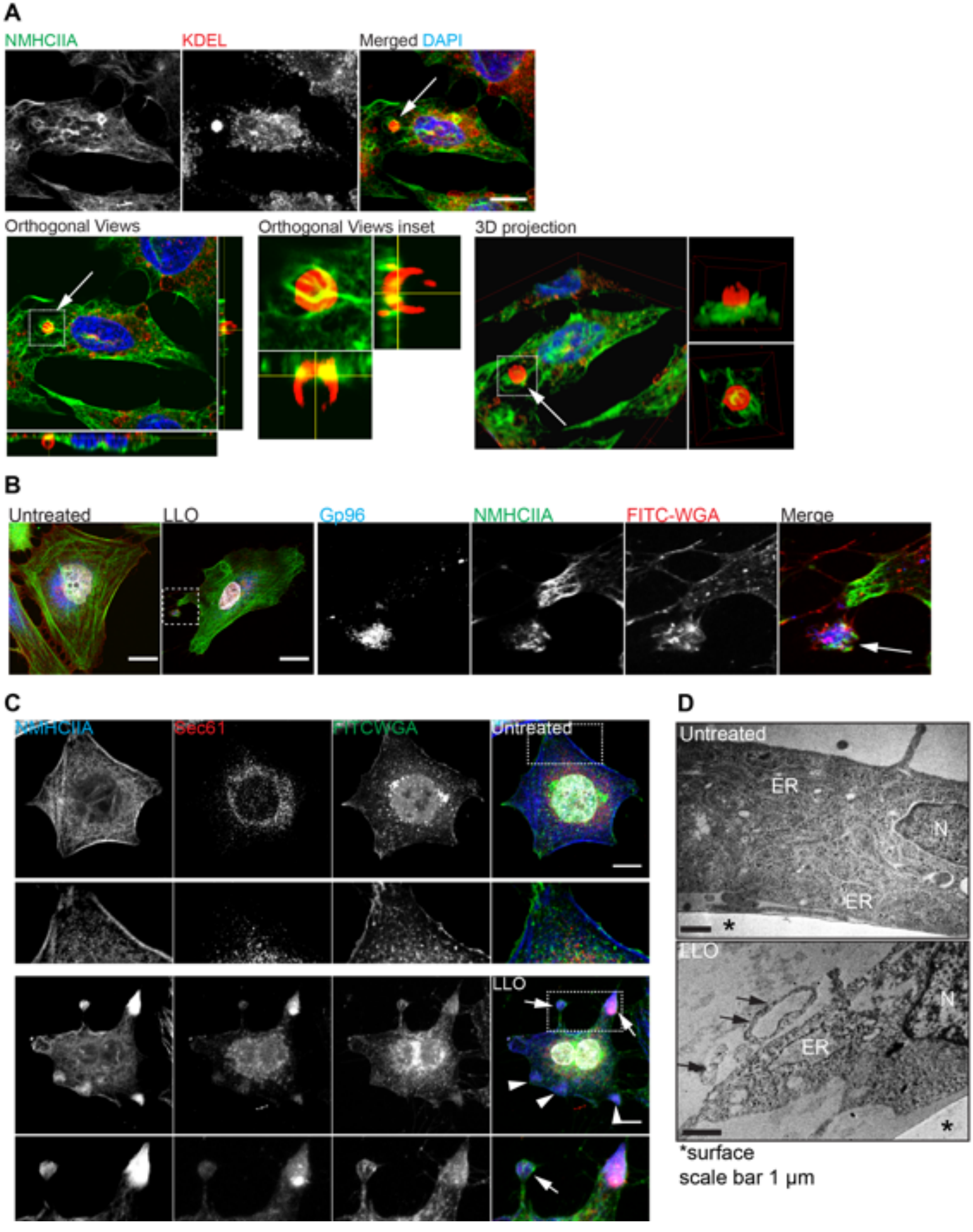


*surface
scale bar 1 μm

Figure 1 – Redistribution of NMHCIIA and ER network upon LLO intoxication